

# **FABRICATION AND CHARACTERIZATION OF ZnO THIN FILM PREPARED BY DIP COATING TECHNIQUE FOR ETHONAL SENSING**

**A Dissertation**

**Submitted to the Dean's Office, Institute of Science and Technology  
Tribhuvan University, Kirtipur in the Partial Fulfillment for the  
Requirements of Master's Degree of Science in Physics.**



**By**

**Jagadish Upadhaya**

**Symbol No.: 1639**

**September, 2021**

## RECOMMENDATION



It is certified that **Mr. Jagadish Upadhaya** has successfully carried out the dissertation work entitled "**FABRICATION AND CHARACTERIZATION OF ZnO THIN FILM PREPARED BY DIP COATING TECHNIQUE FOR ETHONAL SENSING**" under our Supervision and guidance.

We recommend the dissertation in the partial fulfillment for the requirement of Master's Degree of Science in Physics.

.....

(Supervisor)

Mr. Yogesh Singh Maharjan

Assistant Professor

Department of Physics

Amrit Campus

Thamel, Kathmandu, Nepal.

.....

(Supervisor)

Dr. Leela Pradhan Joshi

Professor

Department of physics

Amrit Campus

Thamel, Kathmandu, Nepal.

Date: .....

## **ACKNOWLEDGEMENT**

I would like to express my immense gratitude to my supervisors Professor Dr. Leela Pradhan Joshi and Mr. Yogesh Singh Maharjan, Amrit Campus, Tribhuvan University, for their guidelines, continual direction, encouragement, inspiring me to work independently on this research and encouragement. I significantly appreciate to Assistant Prof. Mr. Pitamber Shrestha (M.Sc. Coordinator) for their persistent inspiration and encouragement. I will always be grateful to Amrit Campus (ASCOL) give me opportunity for doing research. I would also thankful for Assistant Prof Mr. Dinesh Chaudhari for the help of gas sensing. I am also thankful for Meena Shrestha for helping of experiment. I am very much thankful to my friend Jeevan Darai and Preeti Shah as they are always there for my experiment. I would like to remember my friends, who helped me directly or indirectly during this work.

At last, but not the least I would like to thank my appreciation to my parents and wife for their ceaseless support during my time of study and through the way towards exploring and composing this work. Without their care, love and affection, I would never be what I am now.

**Jagadish Upadhaya**

# EVALUATION



We certify that we have read this dissertation work **"FABRICATION AND CHARACTERIZATION OF ZnO THIN FILM PREPARED BY DIP COATING TECHNIQUE FOR ETHONAL SENSING"** and in our opinion, it is good in the scope and quality as a dissertation in the partial fulfillment for the requirement of Master's Degree of Science in Physics.

.....

(Supervisor)

Mr. Yogesh Singh Maharjan

Assistant Professor

Department of Physics

Amrit Campus

Thamel, Kathmandu Nepal.

.....

(Supervisor)

Prof. Dr. Leela Pradhan Joshi

Head of the Department

Department of Physics

Amrit Campus

Thamel, Kathmandu Nepal.

.....

Mr. Pitambar Shrestha

(Assistant Professor)

(Co-ordinator)

Department of Physics

Amrit Campus

Kathmandu, Nepal

.....

(External Examiner)

.....

(Internal Examiner)

Date: .....

## LIST OF ABBREVIATIONS

CVD	Chemical Vapor Deposition
DEA	Diethanolamine
PC	Personal Computer
UV	Ultraviolet
ZnAc	Zinc Acetate
ZnO	Zinc Oxide
A	Energy Constant
$E_g$	Optical Band gap
h	Planck's constant
I	Intensity of radiation
t	Thickness
T	Transmittance
$\alpha$	Absorption Coefficient
$\nu$	Frequency
$\mu$	Micro

## **ABSTRACT**

0.5M Zinc Oxide (ZnO) nano-particle thin films were deposited on cleaned glass substrates by dip coating technique with 350 mm/min dipping speed. These films were optically characterized using UV-Vis spectrophotometer. The band gap of film was found to be 3.11 eV having thickness 903.176 nm. Thickness was measured using a Swanepoel method. The refractive index of ZnO was also measured and its value was found to be 2.091 -1.532 in the wavelength of 350-800 nm. The prepared ZnO thin film was used to detect ethanol vapor in the temperature range 180 to 300 °C. The highest response of 3.4 was found at the operating temperature of 240 °C for 500 ppm of ethanol vapor. Corresponding response and recovery times were found as 9.82 and 16.33 sec respectively.

**Keywords:** ZnO film, Dip Coating, Optical Properties, Sensitivity, Refractive index, Operating Temperature, Ethanol

## List of Figures

Figure 2.1 Schematic Diagram of Dip Coater.....	8
Figure 2.2 Schematic Diagram of Spin Coater .....	9
Figure 2.3 Schematic Diagram of Spray Pyrolysis .....	10
Figure 2.4 Schematic Diagram of Chemical Vapor Deposition.....	11
Figure 2.5 Schematic Diagrams of Magnetic Sputtering .....	12
Figure 2.6 Schematic Diagram of Pulse Laser Deposition .....	13
Figure 2.7 Schematic Diagram of Doctor Blade Methods .....	14
Figure 2.8 Energy Transition in Direct Band Gap .....	17
Figure 3.1 Homebuilt Dip Coating Devices .....	22
Figure 3.2 Muffle Furnace (Nabertherm: 30 °C – 3000 °C) .....	23
Figure 3.3.5 Schematic diagram of process of dip-coating .....	23
Figure 3.4 UV-Vis spectrophotometer (HR4000CG UV-NIR, Ocean Optics) .....	24
Figure 3.5 Envelope on the transmittance curve. T_max and T_min are the fitted curves to the maxima and minima of transmission spectrum .....	25
Figure 3.6 Homemade gas sensor set up.....	26
Figure 4.1 Transmittance for Different Coat of 0.5M with dipping speed 350mm/min. ....	27
Figure 4.2 Transmittance for 0.5 M 7 Coat. ....	28
Figure 4.3 Band Gap of different coat Envelope methods of ZnO thin film with 0.5 M of 7 Coat with speeds 350 mm/min. ....	29
Figure 4.4 Band Gap of 7C coat ZnO .....	29
Figure 4.5 Envelope methods of ZnO thin film with 0.5 M of 7 Coat with speeds 350 mm/min	30
Figure 4.6 Refractive index.....	32
Figure 4.7 Real part of dielectric constant.....	33
Figure 4.8 Imaginary part of dielectric constant.....	34
Figure 4.9 Real and imaginary part of dielectric constant .....	34
Figure 4.10 Working temperature of ZnO thin film for 500 ppm. ....	35
Figure 4.11 Responses and Recovery Time of ZnO sensor at 240°C on 500 ppm.....	36

## List of Tables

Table 3.1 Specification of homebuilt dip coating device .....	21
Table 4.1 Band gaps observed for 0.5M ZnO solutions with variations of different dipping speed and numbers coats.....	30
Table 4.2 The Values of $\lambda$ , T <sub>max</sub> and T <sub>min</sub> obtained from fig4. 5 and the n and d values calculated by Swanepoel method for 0.5M, 7 Coat ZnO thin film.....	31
Table 4.3 The working temperature of ZnO thin film for 7C, 0.5M for 500 ppm ethanol gas vapor. ....	36



## CONTENTS

<b>Contents</b>	<b>Pages</b>
<b>Recommendation</b>	<b>i</b>
<b>Evaluation</b>	<b>ii</b>
<b>Acknowledgements</b>	<b>iii</b>
<b>List of Abbreviations</b>	<b>iv</b>
<b>Abstract</b>	<b>v</b>
<b>List of Tables</b>	<b>vi</b>
<b>List of Figures</b>	<b>vii</b>
<b>Chapters</b>	
<b>1 Introduction</b>	<b>1</b>
1.1 Background	1
1.2 ZnO and Its Applications	3
1.3 Objectives of Research	4
1.4 Literature Review	5
<b>2 Methods of Film Preparation and Characterization Techniques</b>	<b>7</b>
2.1 Methods of Thin Film Preparation	7
2.1.1 Dip Coating	7
2.1.2 Spin Coating	8
2.1.3 Spray Pyrolysis Technique	9
2.1.4 Chemical Vapor Deposition	10
2.1.5 Magnetic Sputtering	11
2.1.6 Pulse Laser Deposition	12
2.1.7 Doctor Blade Methods	13
2.2 Optical Characteristics	14
2.2.1 Optical Properties of Semiconductor	15
2.2.2 Optical Properties of ZnO	15
2.2.3 Thickness Analysis	17
2.2.4 Ethanol Detection Mechanism	19
<b>3 Experimental Details</b>	<b>20</b>
3.1 Introduction	20

3.2 Experimental Setup	20
3.2.1Homemade Dip Coating Set	20
3.2.2Preparation of 0.5M Precursor solution Concentration	21
3.2.3Substrate Cleaning	22
3.2.4 Thin Film Preparation	22
3.2.5 Thin Film Coatings	23
3.3 Sample Characterization	25
3.4 Envelop Method (Swanepoel Method)	25
3.5 Sensitivity Measurements	26
<b>4 Results and Discussion</b>	<b>27</b>
4.1 Optical Properties	27
4.1.1 Transmittance Analysis	27
4.1.2 Band gap Analysis	28
4.1.3 Thickness Analysis	30
4.1.4Refractive Index Analysis	32
4.1.5 Dielectric Constant Analysis	32
4.2 Sensitivity Measurements	35
4.2.1 Working Temperature Measurement	35
4.2.2 Response and Recovery Time	36
<b>5 Conclusions and Future Work</b>	<b>37</b>
<b>References</b>	<b>38</b>

# CHAPTER 1

## INTRODUCTION

### 1.1 Background

Several semiconducting oxides such as SnO<sub>2</sub>, ZnO, In<sub>2</sub>O<sub>3</sub> and indium tin oxide (ITO) are employed as gas sensors, by utilizing the changes of the electrical conductivity of these materials upon exposing to target gases. The utilization of the gas sensors of ZnO has long history. The ZnO gas sensor is used because of the cheapest and easily available at the market. The ZnO has been studied as chemical compound resistance materials to detect gases like H<sub>2</sub>, NH<sub>3</sub>, CH<sub>4</sub>, O<sub>2</sub>, seafood smell, ethanol and CO etc. [1].

The optical properties of the thin film have been studied on the last decades and the great effort has been made to develop the mathematical formulations to describing its transmittance and absorbance. The optical features of semiconductor films depend on different parameters, such as film thickness, deposition rate etc. Our aim here is to investigate the effect of film thickness on the optical properties of ZnO thin films and used as gas sensor. The Swanepoel method has been used on the base of interference fringes of ZnO deposited on glass substrates with refractive index and thickness of higher coats. The proposed Swanepoel's method has been studied with samples of higher coats. In this method origin pro 8.5 was used to calculate the film refractive index and film thickness [2].

The semiconductors such as ZnO, FTO, SnO and so on of thin films have been widely used in the phase-change memories, highly efficient solar cells, on-chip optical circuits, active-matrix display, image sensors, laser-induced films waveguides, photovoltaic devices, etc. Over the past few decades, the optical properties of ZnO films have been the subject of intense study. The accurate knowledge of optical properties (refractive index, transmittance parameter, etc.) of the ZnO films is important for fabricating high-quality optical devices such as gas sensors. Great efforts have been made to study optical properties of the thin films. Many methods have been developed including ellipsometry, fitting method, reflection spectrum. The most common method was proposed by Swanepoel. In this method the refractive index, thickness etc of the films are calculated from their transmission spectrum. In Swanepoel method researchers have

presented some different analytical algorithms for determining the thickness and optical parameters of the thin films [5].

In present days, detection and controls of volatile organic compounds (VOCs) in atmosphere emitted by textile, paint, pesticide, medical, fragrance and food processing industries has been a major concern for scientist and engineers. The presence of toxic and carcinogenic VOCs in environments will have severe health impacts and lead to premature death. In this scenario, one of the most versatile VOCs namely ethanol being a low-cost alternative fuel and industrial solvent has major threat to the environment. Discharging of excess concentration of ethanol in atmosphere may create skin and eye irritation, nausea and vomiting, central nervous system depression and acidosis. Hence, to detect and control the ethanol concentration in environment has emerged as a new challenge to avoid such health risks. In this context, metal oxide gas or VOC sensors will have to play a prominent role to detect ethanol in the atmosphere. Among the various metal oxide materials, zinc oxide (ZnO) has become a potential compound because of its versatile and tunable nature [6, 7].

Nano materials are unique because of their mechanical, optical, electrical, catalytic and magnetic properties. Apart from this, these materials also possess high surface area per unit mass. Further, new physical and chemical properties emerge when particles are in nanometer scale. The specific surface area as well as surface to volume ratio increase drastically when the size of the material decreases. Also, the movement of electrons and holes in semiconductor nanomaterials are affected by size and geometry of the materials. High crystalline structure, ability of noble metal doping, and competitive production rate increase the demand of production for nanoparticles for gas sensors development. The gas sensing properties of zinc oxides, depend naturally on their catalytic or surface chemical properties as well as on their physical or morphological properties. Furthermore, most of the reactions involved in the detection of gases rely on the reaction between the adsorbed oxygen and the test gas, so that the working temperature is usually quite high [8, 9].

## 1.2 ZnO and Its Applications

Among the various metal oxide semiconductors Zinc oxide (ZnO) is chemically and thermally stable n-type semiconductors with a large excitation binding energy of 60 meV and large band gap energy of 3.37 eV at room temperature [10]. ZnO is applied in various applications such as gas sensors, dye-synthesis solar cell, and light emitting diode (LED) [11, 12]. ZnO is known to be one of the widely applied oxide gas sensing materials [13]. Gas sensing elements have been fabricated in various forms, including single crystals, sintered pellets, thick films, thin films and hetero-junctions. The gas sensing mechanism involves absorbing a substance of oxygen on the oxide surface followed by charge transfer during the reaction between chemisorbed oxygen reducing and target gas molecules. The ZnO thin film can be fabricated at low cost and are widely compatible to microelectronic technology and circuits. Some dangerous and poisonous gases, e.g., hydrogen, LPG, carbon monoxide and methane, etc., could be detected using ZnO sensors. For increasing gas sensing properties of the sensors, some metal ions were considered to dope in the zinc oxide [14].

Many methods have been used to deposit ZnO films on different substrates including sol-gel processes, spray pyrolysis, metal organic chemical vapour chemical deposition (MOCVD) , pulsed laser deposition (PLD), molecular beam epitaxial (MBE), sputtering . Spray pyrolysis has been developed has a powerful tool to prepare various kind of thin film such as metal oxides, superconducting materials and nano phase materials. In comparison to others spray pyrolysis has several advantages such as high purity, excellent control of chemical uniformity in multi-component system [15].

Detection and monitoring of flammable, toxic and exhaust gases are important for both energy saving and environmental protection [16]. The cheap, reliable, small and low power-consuming gas sensors are in great demand due to the wide range of applications. With the increasing demand of gas sensors of higher selectivity and sensitivity, rigorous efforts are in progress to find more suitable material with required surface and bulk properties. Semiconductor metal oxide (SMO) gas sensors are the most investigated group of gas sensors and recently the SMOs, having size in the range of 1 nm–100 nm [17] , are being increasingly used for gas sensing due to their size dependent properties. The specific surface area as well as surface to volume ratio increase drastically when the size of the material decreases [18]. Zinc oxide thin films doped

with various materials such as Fe, Cu and Al have been widely explored for the development of selective gas sensors [19].

Moreover, ZnO is a typical chemical compound sensing material. Its gas sensing is dominantly controlled by the change in sensor resistance when gas molecules react to its surface [19]. In ambient atmosphere, oxygen molecules are adsorbed on the surface of ZnO and then ionize into oxygen species by capturing electrons from the conduction band, leading to the formation of surface depletion layer and thus increasing the sensor resistance [20]. ZnO is the most important group ii-vi semiconductor materials. It is the typical semiconductor which is important for the electronic and photonic material for a wide range of technological applications in devices including surface acoustic wave filters, chemical sensors, transparent conductors, light-emitting diodes and optical modulator wave-guides [21].

### **1.3 Objectivity of Research**

The objectives of this research works are set below;

1. To fabricate the ZnO thin films on the glass substrates.
2. To study the optical properties of these thin films.
3. To design the gas sensor setup & measure sensitivity of the prepared ZnO thin films.

#### 1.4 Review of literature

In this topic, we reviewed so many articles and research papers related to these topics.

E. R. Shaban group has been studied validity of Swanepoel methods for calculating the optical constant for thick films. In their study amorphous  $\text{Ge}_{25}\text{Cd}_5\text{Se}_{70}$  film has been used on glass substrate by using thermal evaporation process methods. Interference fringe pattern has been used to derive the refractive index and film thickness in  $\mu\text{m}$  range and band gap has been studied that 1.915 to 1.975 eV of different thickness, envelop methods suggested by Swanepoel has been applied [3].

Y. Jain and group has used Swanepoel method for deriving the thickness and the optical properties of chalcogenide thin films. In this study a tangency point method (TPM) is presented to derive the thickness and optical constants of chalcogenide thin films from their transmission spectra. They solved the problem of the abnormal value of thickness in the strong absorption region obtained by Swanepoel method also found the thickness and refractive index is better than 0.5%. They compared with Swanepoel method by using the same simulation and experimental data from the transmission spectrum, the accuracy of the thickness and refractive index obtained by the TPM is higher in the strong absorption region [4].

Nadir F. Habubi and group studied optical parameters of amorphous selenium deposited by thermal evaporation technique. In this study thin films of amorphous selenium have been prepared by thermal evaporation technique. The analysis proposed by Swanepoel has been successfully employed to determine the average thickness and refractive index of the films with high accuracy in the spectral range of 540-1050 nm. They also found that absorption coefficient  $\alpha$ , therefore extinction coefficient  $k$  determined from the transmission spectra at the strong absorption region, the optical absorption edge is described using Tauc formula and found that the transition was direct with an energy gap equal to 2.02 eV [5].

Mehmet Can Akgun group has studied the hydrothermal zinc oxide nanowires growth using zinc acetate dihydrate salt with the effect of time, temperature, and solution concentration on growth process of nanowires. In their study, ZnO film were deposited on silicon (001) substrate using spin coating method. In their study they used Zinc acetate dehydrate and 1-propanal of chemicals were using seed layer were dipped in to aqueous solution of zinc acetate dehydrate and

hexamethylenetetramine at set temperature and kept for desired duration for time for growth. In their experiments the nanowires found to be controlled by precursor concentration [22].

Naif Ahmed Alshehriet al., studied hydrothermal growth of ZnO nanowires for scale up applications with the effect of growth duration time, base concentration ( $\text{Na}_2\text{CO}_3$ ). zinc chloride, zinc nitrate hexahydrate, zinc acetate dihydrate and sodium carbonate chemicals were used as precursor materials. The process was taken place inside a 125 mL Teflon vessel in an autoclave placed inside oven at 140 °C for 2-26 hour. Finally dry power was sonicated in DI for ultrasonic bath for 10 min. [23].

C.S. Prajapati and P.P. Sahay 2011 have studied Alcohol-Sensing characteristics of Spray deposited ZnO nano-particles thin films. Structural and morphological studies were studied zinc acetate dihydrate and DI chemicals were used. They also studied the sensing characteristics on statistic system. They found ZnO nano particle of size 25 nm, selective high response on alcohol sensing mechanism [24].

ZnO nanowires were grown hydrothermally on seed layer of ZnO thin film deposited by spin coating and dip coating method which were studied by Yang, Wan and Chen in 2009. Prepared ZnO nanowires were used to assemble DSSCs. In order to further investigate, the effect of  $\text{TiO}_2$  buffer layer on ZnO nanowires based DSSC were compared with the ZnO nanowires based DSSC with FTO. They found from  $\text{TiO}_2$  layer the photovoltaic conversion efficiency & open circuit voltage of ZnO nanowires based DSSCs were improved by 3.9-12.5% and 2.4-41.7% respectively [25].

Mohammed M. Rahman group has studied fabrication of smart chemical sensors based on transition-doped-semiconductor nanostructure materials with  $\mu$ -chips on  $\text{Sb}_2\text{O}_3$  doped ZnO MFs. F. In their study zinc chloride, antimony chloride, ammonium hydroxide and DI chemicals were used. They found that the simple fabricated and displayed higher chemical sensitivity for ethanol [26].



## **CHAPTER 2**

# **METHODS OF FILM PREPARATION AND CHARACTERIZATION TECHNIQUES**

### **2.1 Methods of Thin Film Preparation**

There are various methods for the deposition of thin films on the glass substrates. Some of them are: Dip coating, Spray-pyrolysis, Spin-coating, Chemical vapor deposition, Magnetic sputtering, Pulse laser deposition and Doctor Blade methods.

#### **2.1.1 Dip Coating**

Dip coating is one of the most widely adopted, simplest processes used for the deposition of thin film on the glass substrates for the synthesis of thin or thick films of Zinc Oxide, Tin Oxide etc.

In this method easily improve the efficiency of sensors, easy control over the thickness of the film, a good homogeneity, can be used for large coating areas, low-cost technique and finally it is also a low temperature operating process. Dip coating process is generally applicable for flat or cylindrical surfaces [27].

First of all, the substrate is immersed into the precursor solution containing the coating materials at constant speed, where it remains there for some time. It is then taken out at constant speed. The thin layer is deposited on the surface of the substrate, whose thickness is determined through the pulled-up speed. The coating thickness increases with the increase in the pulling up speed. Finally, the coatings are annealed in order to evaporate the solvent, which results in the formation of thin layer [28].

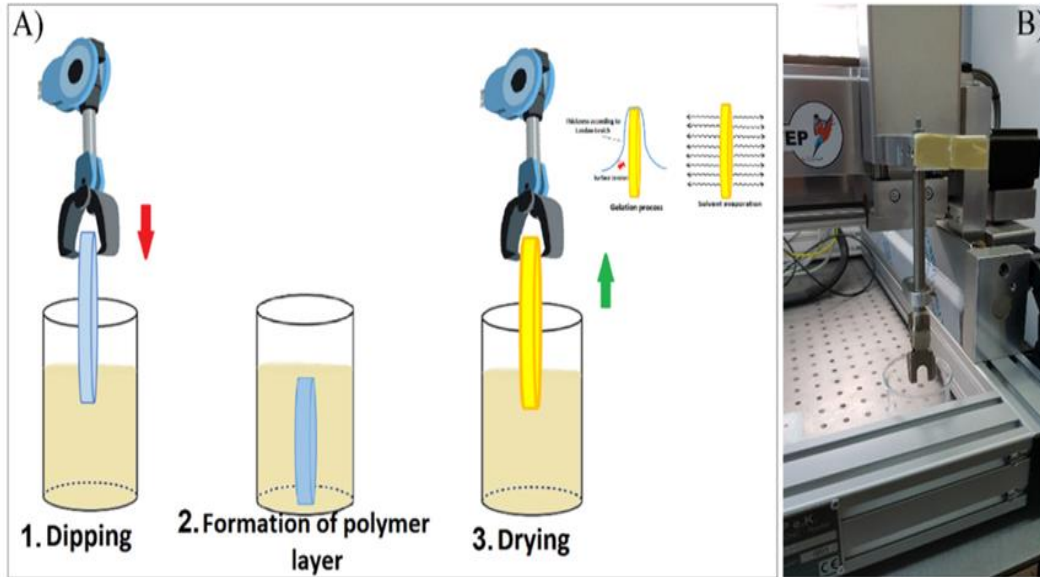


Figure 2.1 Schematic diagram of a Dip Coater [28]

### 2.1.2 Spin Coating

Spin coating technique is another one of the most widely adopted, simplest processes used for the deposition of thin film on the glass substrates. This method is simple, low cost. Using this method, we can control the film thickness and repeatability. A small amount of coating material is applied at the center of the substrate, which is spinning at constant speed. The substrate is rotated at high speed so as to spread the coating material all over the substrate. When the coating is finished, the substrate is heated for the evaporation of unwanted solvent. The process is repeated until the desired thickness is achieved. It is the method of centrifugal deposition. It is widely used in micro-fabrication, where it can be used to create thin films with thickness below 10nm. It is used intensively in photolithography, to deposit layers of photo resist about 1 micro meter.

The main parameters of the spin coating system are spinning time, angular speed of the spin, concentration of the solution, its viscosity etc. [29, 30].

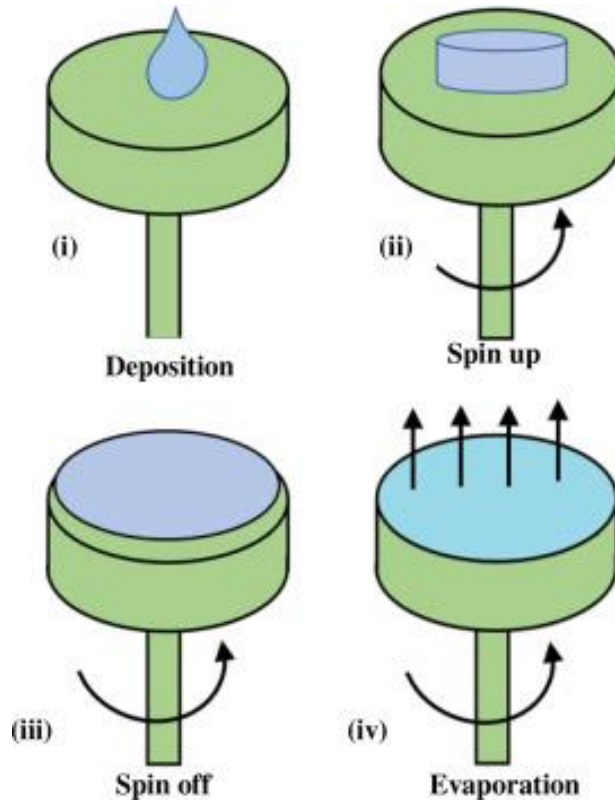


Figure 2.2 Schematic diagram of a Spin Coater [30]

### 2.1.3 Spray Pyrolysis Technique

Spray pyrolysis technique is also one of the simplest processes in which a thin film is deposited by spraying solution on a hot surface. This process is used in depositing thin films that can be used in devices such as solar cells, sensors, solid oxide fuel cells etc. The prepared film deposited from this technique has high purity; one can control the chemical uniformity of the film. The spray pyrolysis technique consists of: Heater, Substrate, Thermocouple, Pressure Regulator, Solution, Spray Nozzle and Android system hotspots [31].

The spray gun is used to spray the precursor solution onto the glass substrate. The solution is sprayed in the form of mist. Heater is used to heat the substrate and the temperature is maintained using thermocouple. The precursor solution is sprayed through the spray gun at constant rate, which results in the formation of uniform thin film. We can control the electrical, structural, adherence, optical and surface morphology of the thin film by proper selection of the substrate, starting solution and optimizing the conditions like substrate temperature, flow rate of

the solution, concentration of the solution, spray time, etc. [32]. Describe figure below with figure number.

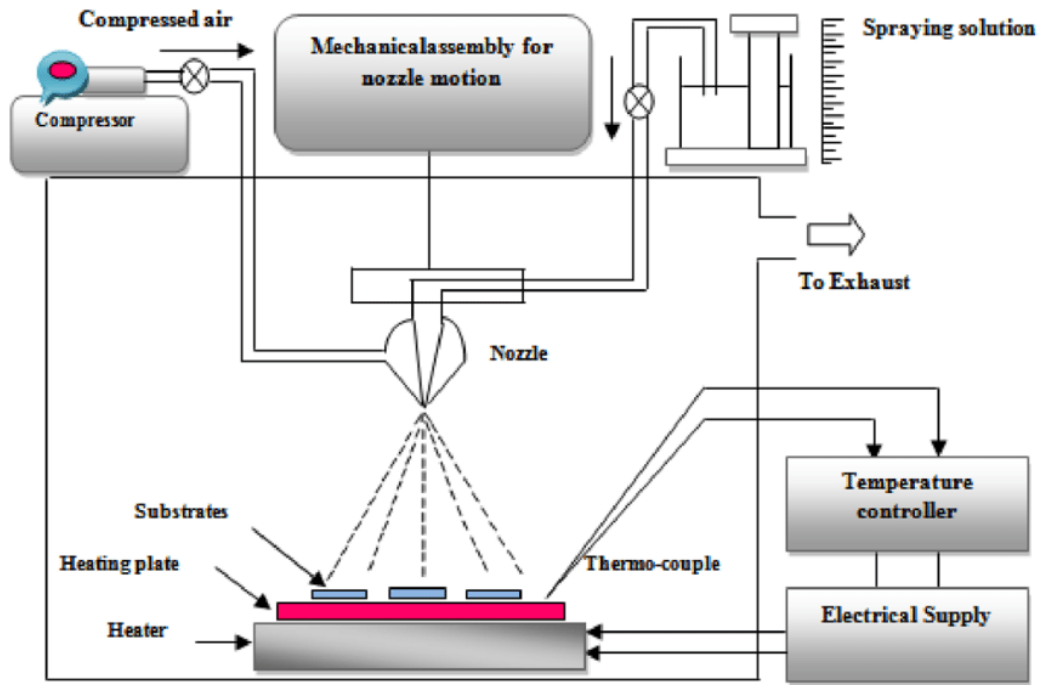


Figure 2.3 Schematic diagram of a Spray Pyrolysis [33]

#### 2.1.4 Chemical Vapor Deposition

Chemical Vapor Deposition (CVD) is most widely used method of synthesis of thin film in the semiconductor industry. It consists of a reaction chamber containing the substrate at suitable temperature. The precursor gas is allowed to pass through the chamber. The gas decomposes to form the thin layer of film since it is in contact with the heating substrate. It can also be stated as the coating material is heated until vaporizes. So, the material begins to settle onto the substrate and form a uniform coating. We can control the thickness of the coatings by simply adjusting the temperature and duration of the process [34]. Describe figure below in your own words.

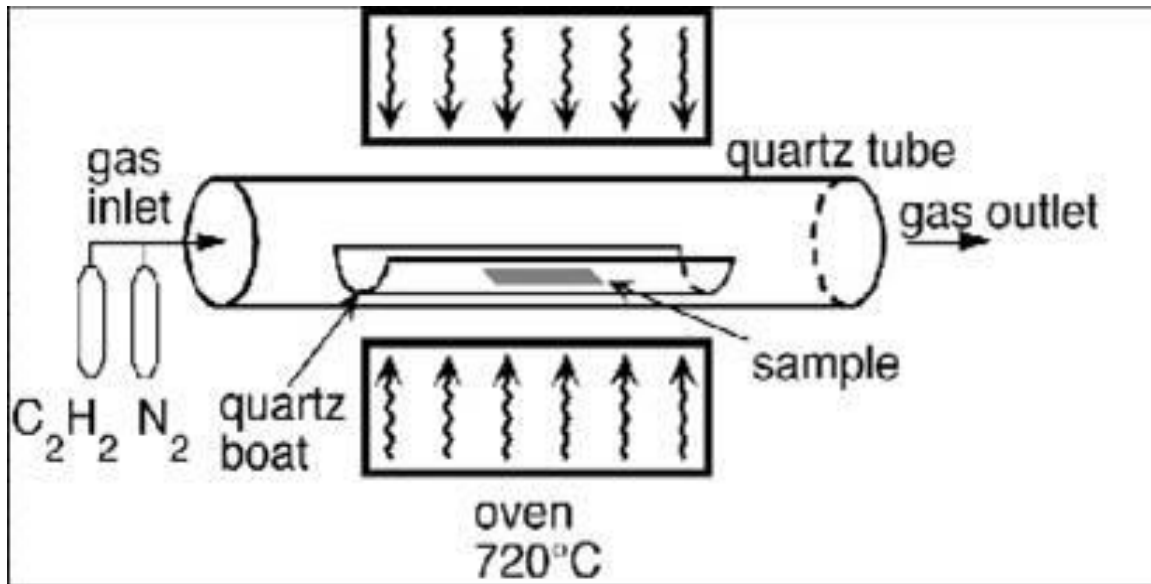


Figure 2.4 Schematic diagram of Chemical Vapor Deposition [34]

### 2.1.5 Magnetic Sputtering

It is a physical vapor deposition (PVD) process. The thin film is deposited on the substrate by ejecting the atoms from a solid target material due to bombardment of the target by energetic ions. It happens when the kinetic energy of the incoming particles is much higher than conventional thermal energies. The inert gas such as Argon is usually used in this method. There are various types of sputtering process, they are:

Reactive Sputtering, High-Target-Utilization Sputtering, Ion-Assisted Deposition, High- Power Impulse Magnetron Sputtering (HIPIMS) and Gas Flow Sputtering [35].

Describe in a paragraph figure below.

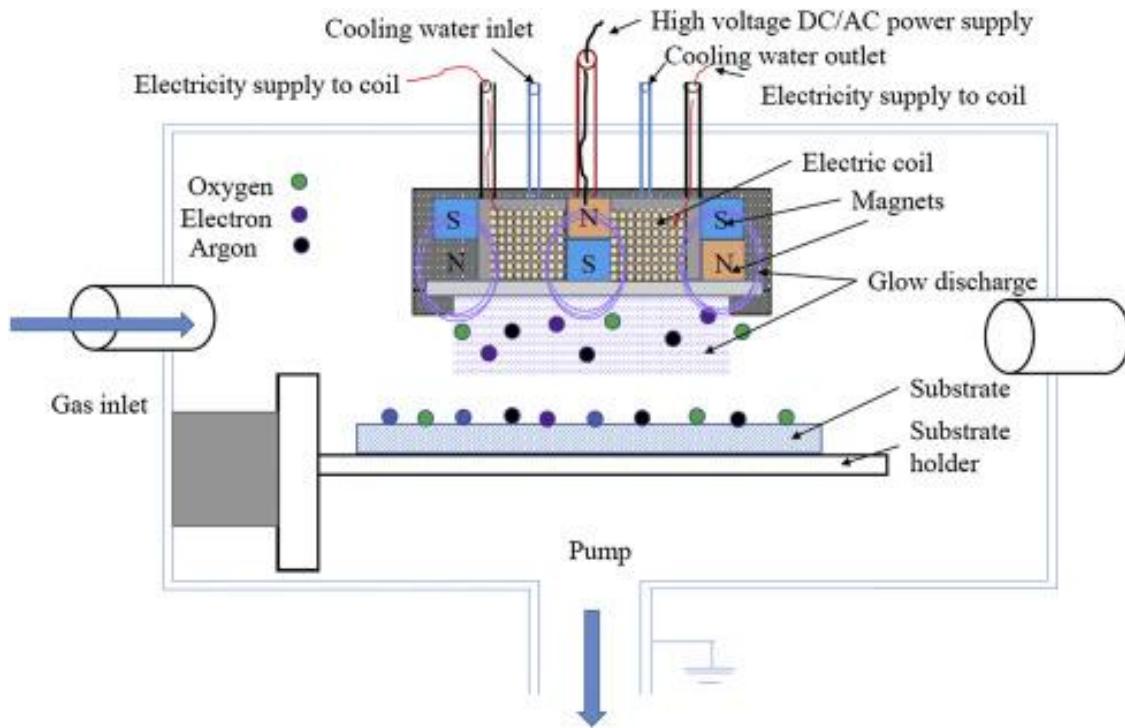


Figure 2.5 Schematic Diagrams of Magnetic Sputtering [35]

### 2.1.6 Pulse laser Deposition

Pulse laser deposition (PLD) is a physical laser deposition technique, where a high-power pulse laser beam strikes the target inside a vacuum chamber. It utilizes the plasma resulting from the interaction of focused laser radiation pulses with the target surface to deposit thin film coatings composed of one or more target materials. Although its basic setup is simple, it is not used for the deposition of thin film in our research as the growth of the film as well as the physical phenomena of laser-target interaction is indeed complex. The main advantages of this technique are: Conceptually simple: a laser beam vaporizes a target surface, producing all film with the same composition as the target, Versatile: many materials can be deposited in all wide variety of gases over a broad range of gas pressure, Cost-effective: one laser can serve many vacuums system and fast high-quality samples can be grown reliably in 10 or 15 minutes [36].

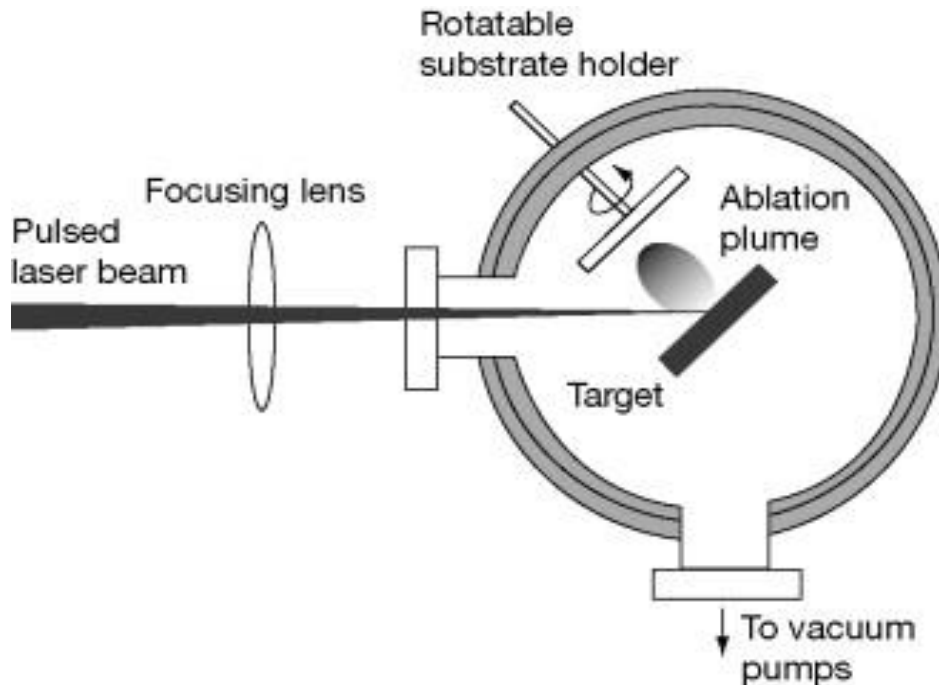


Figure 2.6 Schematic Diagram of Pulse Laser Deposition [36]

### 2.1.7 Doctor Blade Methods

This method is also one of the widely used techniques for producing thin films on large area surfaces. Tape casting is a relatively new process which was originally developed during the 1940's as a method of forming thin sheets of piezoelectric materials and capacitors. It is now an accepted precision coating method. In the doctor blading process, a well-mixed slurry consisting of a suspension of particles along with other additives is placed on a substrate beyond the doctor blade. When a constant relative movement is established between the blade and the substrate, the slurry spreads on the substrate to form a thin sheet which results in a gel-layer upon drying. The doctor blading can operate at speed up to several meters per minute and it is suitable to coat wet film thicknesses ranging from 20 to several hundred microns. There are two generally different coating devices in use: a doctor blade (e.g., a rectangular frame) and a spiral film applications [37].

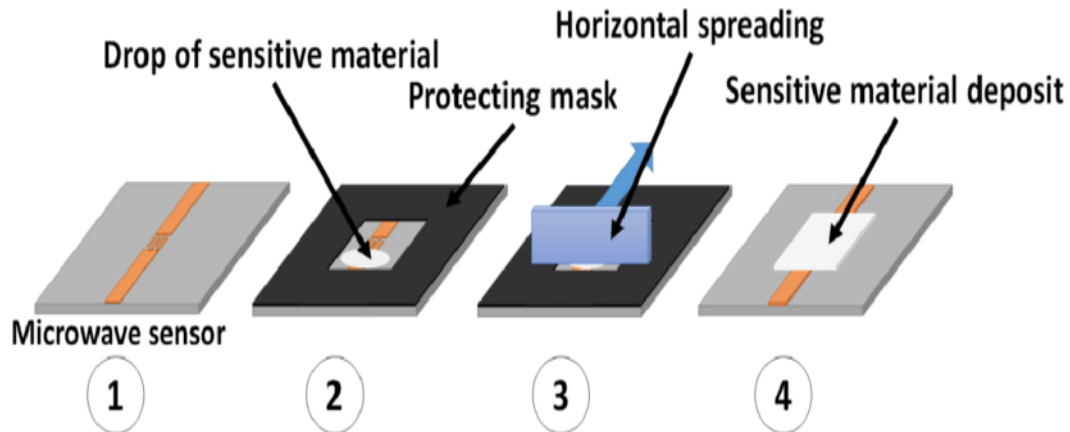


Figure 2.7 Schematic diagram of a Doctor Blade methods [37].

## 2.2 Optical Characteristics

ZnO is a key technological material. ZnO is a wide band-gap (3.37 eV) compound semiconductor that is suitable for short wavelength optoelectronic applications. The high exciton binding energy (60meV) in ZnO crystal can ensure efficient excitonic emission at room temperature. R room temperature ultraviolet (UV) luminescence has been reported in disordered nanoparticles and thin films. In addition, the lack of a center of symmetry in quartzite, combined with large electromechanical coupling, results in strong piezoelectric and pyroelectric properties and the consequent use of ZnO in mechanical actuators and piezoelectric sensors. Furthermore, ZnO is a versatile functional material that has a diverse group of growth morphologies, such as nanocombs, nanorings, nanohelices/nanosprings, nanobelts, nanowires and nanocages. These ZnO nanostructures are easily formed even on cheap substrates such as glass and hence they have a promising potential in the nanotechnology future. Finally, ZnO nanostructures are also attractive for biomedical application since it is a bio-safe material and its nanostructure has a large surface area [38]. As well as we know, all these applications definitely originate from its basic properties. Therefore, in order to in-depth know about ZnO, the structural and optical properties of ZnO will be introduced in detail in these chapter. Optical properties and processes in ZnO as well as its refractive index were extensively studied many decades ago. The renewed interest in ZnO is fueled and fanned by its prospects in optoelectronics applications owing to its direct wide band gap of 3.37 eV at room temperature with large exciton energy of 60 meV and efficient radiative recombination. The strong exciton binding energy, which is much



larger than that of GaN (25 meV), and the thermal energy at room temperature (25 meV) can ensure an efficient exciton emission at room temperature under low excitation energy. As a consequence, ZnO is recognized as a promising photonic material in the blue-UV region [39].

### **2.2.1 Optical properties of semiconductor**

The optical properties of a semiconductor have their genesis in both intrinsic and extrinsic effects. Intrinsic optical transitions take place between the electrons in the conduction band and holes in the valence band, including excitonic effects due to the Coulomb interaction. Excitons are classified into free and bound excitons. In high quality samples with low impurity concentrations, the free excitons can also exhibit excited states, in addition to their ground-state transitions. Extrinsic properties are related to dopants/impurities or point defects and complexes, which usually create electronic states in the band gap, and therefore influence both optical absorption and emission processes. The electronic states of the bound excitons, which may be bound to neutral or charged donors and acceptors, depend strongly on the semiconductor material, in particular the band structure. For a shallow neutral donor bound exciton, for example, the two electrons in the bound exciton state are assumed to pair off into a two-electron state with zero spin. The additional hole is then weakly bound in the hole-attractive Coulomb potential set up by this bound two-electron aggregate. Similarly, neutral shallow acceptor bound excitons are expected to have a two-hole state derived from the topmost valence band and one electron interaction. Other extrinsic transitions could be seen in optical spectra such as free-to-bound (electron acceptor) and bound-to-bound (donor-acceptor) [38].

### **2.2.2 Optical properties of ZnO**

Optical transitions in ZnO have been studied by a variety of experimental techniques such as optical absorption, transmission, reflection, photo reflection, spectroscopic ellipsometry, photoluminescence, cathode luminescence, calorimetric spectroscopy, etc. It is well known that at room temperature the PL spectrum from ZnO typically consists of a UV emission band and a broad emission band, as shown in Figure 2.5. The UV emission band is dominated by the free exciton (FE) emission. The broad emission band literally between 420 and 700nm observed nearly in all samples regardless of growth conditions is called deep level emission band (DLE) [39].

The UV emission band is related to a near band-edge transition of ZnO, namely, the recombination of the free excitons. The deep level emission band has previously been attributed to several defects in the crystal structure such as O-vacancy (VO), Zn-vacancy (VZn), O-interstitial (Oi), Zn-interstitial (Zni), and extrinsic impurities such as substitutional Cu. Recently, this deep level emission band had been identified and at least two different defect origins (VO and VZn) with different optical characteristics were claimed to contribute to this deep level emission band [40].

When the light of suitable frequency falls on the semiconductor, some of the light gets reflected, some are transmitted while remaining lights gets absorbed. The conductivity of the semiconductor is affected by the absorption of light. The band gap of the semiconductor is smaller than that of the insulator & is considered as the energy gap where no electrons exist. The band gap is defined as the difference between the top of the valence band called valence band edge and the bottom of the conduction band called conduction band edge. The conduction of the electron takes place when the semiconductor absorbs energy equal to or more than the band gap energy. There are two types of band gaps: (1) Direct band gap and (2) Indirect band gap [42].

If the K-vectors in semiconductor are same, then the band gap is called the direct band gaps and if they are different, it is called indirect band gaps. In direct band gap, the momentum of the electrons and holes lie in the same edge in both conduction band and the valence band. The absorption takes place if  $h\nu = E_g$ , where,  $E_g$  is the band gap energy. The optical absorption coefficient ( $\alpha_{hv}$ ) is given by

$$\alpha_{hv} = A(h\nu - E_g)^{\frac{1}{2}} \quad (2.1)$$

Where, A is the constant,  $h\nu$  is the photon energy of incident light and  $E_g$  is the band gap.

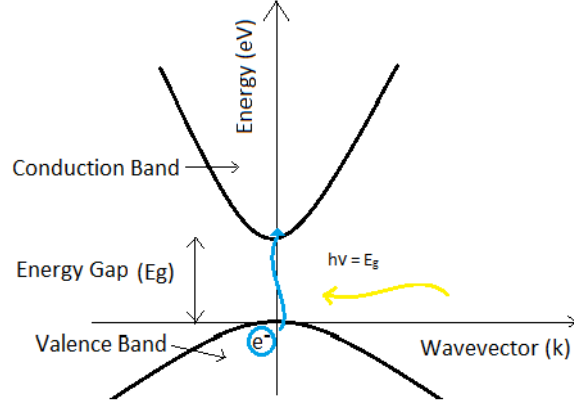


Figure 2.8 Energy transition in direct band gap [43]

The electrons pass through the intermediate state in the case of indirect band gap and transfer momentum to the crystal lattice. In indirect band gap, the optical absorption is given as,

$$\alpha h\nu = A(h\nu \pm E_p - E_g)^n \quad (2.2)$$

Where, A is constant,  $E_p$  is photon energy and n are the number which is equal to 2 for indirect allowed transition and 3 for indirect forbidden transition.

If  $I_0$  be the intensity of incident radiation to the material of thickness 't', then, the intensity of the energy radiation is given as:

$$I = I_0 e^{-\alpha t} \quad (2.3)$$

$$\ln\left(\frac{I}{I_0}\right) = -\alpha t \quad (2.4)$$

This is known as Lambert-Beer's Law.

Where,  $\alpha$  be the absorption coefficient and  $\alpha t$  is called the optical density or absorbance.

The Transmittance can be written as:

$$T = \frac{I}{I_0} = e^{-\alpha t} \quad (2.5)$$

And the absorbance is:

$$A = \ln\left(\frac{1}{T}\right) \quad (2.6)$$

$$A = \ln\left(\frac{I_0}{I}\right) = \alpha t \quad (2.7)$$

Where, T and A are the transmittance and absorbance respectively. We can determine the absorption coefficient of the material by plotting the absorbance or transmittance with different wavelength [17].

### 2.2.3 Thickness Analysis

Thickness of the deposited film is an important parameter to be calculated to study the semiconductor. By knowing thickness, we can calculate many other parameters such as, absorption coefficient ( $\alpha$ ), reflection coefficient, transmittance (T), refractive index ( $\mu$ ) etc. The measurement of the thickness of film is not easy by commonly available methods. The thickness of thin film can be calculated by using envelope methods suggested by Swanepoel applied to the film with higher thickness or maximum coat. By taking the account of two consecutive curves in the Transmittance spectra. Consider the two prominent peaks of T % versus the wavelength for maxima and minima have been calculated by using following formula [3, 4, 5 ].

Now refractive index for glass substrate,

$$s = 1.533 \quad [3] \quad (2.8)$$

$$n = \sqrt{(N + (N^2 - s^2)^{\frac{1}{2}})} \quad (2.9)$$

Where;

$$N = 2s \left[ \frac{T_{max} - T_{min}}{T_{max}T_{min}} \right] + \frac{s^2 + 1}{2} \quad (2.10)$$

Where,  $T_{max}$  and  $T_{min}$  are maximum and minimum transmittance at the corresponding wavelength. $\lambda$ .

Further, refractive index for two consecutive peaks is

$$n_1 = \sqrt{(N_1 + (N_1^2 - s^2)^{\frac{1}{2}})} \quad (2.11)$$

And,

$$n_{12} = \sqrt{(N_2 + (N_2^2 - s^2)^{\frac{1}{2}})} \quad (2.12)$$

Where;

$$N_1 = 2s \left[ \frac{T_{M_1} - T_{m_1}}{T_{M_1}T_{m_1}} \right] + \frac{s^2 + 1}{2} \quad (2.13)$$

And,

$$N_1 = 2s \left[ \frac{T_{M_2} - T_{m_2}}{T_{M_2}T_{m_2}} \right] + \frac{s^2 + 1}{2} \quad (2.14)$$

From the calculation,

Now the thickness is calculated by following formula

$$d = \frac{\lambda_1 \lambda_2}{2(\lambda_1 n_2 - \lambda_2 n_1)} \quad (2.15)$$

Is for the respective maxima or maxima and minima or minima

For the calculations of  $m_0$ ,  $d_2$ , and  $n_2$  as using formula as

$$2d_1(\text{avg}) = m_0 \lambda \quad (2.16)$$

Where, m is integral multiple of maxima and half-integral multiple of minima.

For the calculation of,  $m_0$ ,

$$m_0 = \frac{2d_1(\text{avg})}{\lambda} \quad (2.17)$$

Again, for  $d_2$

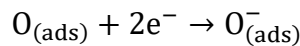
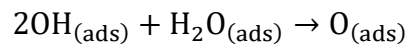
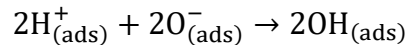
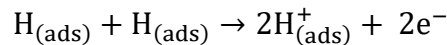
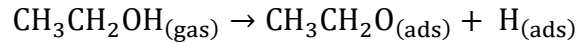
$$d_2 = \frac{m \cdot \lambda}{2n_1} \quad (2.18)$$

Also, for  $n_2$  also

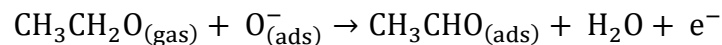
$$n_2 = \frac{m_0 \lambda}{2d_2(\text{avg})} \quad (2.19)$$

## 2.2.4 Ethanol Detection Mechanism

The mechanism of ethanol oxidation over ZnO surfaces have been studied [32]. First of all, ethanol dehydrogenates to form the acetaldehyde ( $\text{CH}_3\text{CHO}$ ) intermediate & forms adsorbed hydrogen atom. The adsorbed hydrogen atom is then oxidized by ZnO surfaces. It generates the protons forming  $\text{OH}_{(\text{ads})}$ . The two adsorbed OH groups condense and remove one  $\text{H}_2\text{O}$  molecules, one net electron is released during this process into the conduction band of ZnO, and thus it reduces its resistance. The overall reaction involved in this mechanism is given below



The above reactions can be summarized as:



# CHAPTER 3

## EXPERIMENTAL DETAILS

### 3.1 Introduction

In this chapter, we mainly focus on the fabricating and characterize thin film of ZnO on the glass substrate. We also deal with the construction of sensor setup for the measurement of sensitivity. The film preparation process is explained in first segments and sensor setup on second segments respectively.

### 3.2 Experimental Setup

There are various methods for the preparation of thin films, the dip-coating methods is chosen for this research because, it is the most widely used, low costing, uniformly coated and easily control for doping concentration, thickness etc.

#### 3.2.1 Homemade Dip Coating Technique

Dip coating is one of few techniques that allow a simultaneous double-sided coating of flat substrates. The wet chemical sol-gel processing is the versatility and ease of liquid film deposition techniques; hence dip coating process is particularly suited for coating flat (glass slide) rigid substrates, but also more complex geometries can be coated with modified techniques. The coating thickness can be controlled basically by the withdrawal speed and by the concentration and viscosity of the coating liquid. For a given coating system, however, there is normally an operational range that allows the preparation of smooth and homogeneous films. The homebuilt dip coater's in-built software (no PC required) is fully automated, which allow coating independent with different withdrawal speed and dwelling time. This device has two switches, which stop the forward and backward movement preventing from the crashing of the substrate into a beaker, saving the user from damaging sample. The parameter of this device is air holding time (sec), dipping time (sec) and speed (mm/min).

Table 3.1 Specification of homebuilt dip coating device

Minimum Withdrawal Rate	1 mm/min
Maximum Withdrawal Rate	399 mm/min
Minimum Dipping Time	1 sec
Maximum Dipping Time	300 sec
Minimum Air Holding Time	1 sec
Maximum Air Holding Time	600 sec
In-built Software Features	Variable withdrawal speed Repeat cycles Crash detection switches/ limiting switches
Program	Costumed Arduino microcontroller
Power Supply	12 V DC
Display	LCD display
Overall Product Dimensions	Height: 45 cm Breadth: 15 cm Main Structure: Ply Board
Weight	3.2 kg

### 3.2.2 Preparation of 0.5M Concentration

0.5M precursor solution was prepared by taking 4.390 gm of Zinc Acetate dihydrate in a beaker dissolved in 40 ml of ethanol. 2.102 gm of Diethanolamine (DEA) was added in the solution. The molar ratio of Zinc Acetate and DEA was maintained as 1:1. The DEA was used as the stabilizer in the solution. The solution was mixed and stirred using Magnetic stirrer (Daihan Scientific Co., Ltd.: MSH-20D), at 60°C for 1 hour. The solutions filtered using WHATMANN filter paper.

All prepared solutions were aged for 4 months in order to check whether precipitation was formed or not, if ppt. was seen, and used for coatings.

### 3.2.3 Substrate Cleaning

Before the thin film preparation and deposition on glass substrate, very important to cleaning glass substrate, to made sample of smoothness, purity, uniformity and porosity. For this glass substrate were first cleaned and wash with detergent and tap water to remove dust and cleaned

with de-ionized water and glass substrate were dried at hot oven at 100 degrees at 1 hour. Finally, glass substrate is ready to film deposition.

### 3.2. Thin Film Preparation

Thin films of ZnO were coated on the glass substrates of dimensions (2.6x7.6x0.1) cm<sup>3</sup> using dip coater. It has different speed per minutes as 1 mm/min to 399 mm/min but I choose the speed as 50 mm/min, 150 mm/min, 250 mm/min and 350mm/min for the thin film coatings. A picture of the spin- coater is shown in figure 3.1.



Figure 3.1 Homebuilt Dip Coating Device [At Amrit research lab]

0.1M, 0.3M and 0.5 M concentrated precursor solution was prepared by using following chemicals:

Zinc Acetate dihydrate [Zn (CH<sub>3</sub>COOH)<sub>2</sub>·2H<sub>2</sub>O] (Qualigens Fine Chemicals, Minimum assay: 98.5 %), Ethanol (AR Grade, Minimum assay: 99.9 %), Diethanolamine (DEA)[C<sub>4</sub>H<sub>11</sub>NO<sub>2</sub>] (Fisher Scientific, Minimum assay: 98.0 %)

All chemicals used were of AR grade. The weight of the chemicals was taken using digital balance with precision of 1mg (PHOENIX: WA3203NJ).

#### 3.2.5 Thin Films Coatings

The glass substrates were used to dip-coater at different speeds as 50mm/min, 150 mm/min, 250 mm/min, and 350 mm/min. Doping glass substrate on the seed layer the first of all fixed air



holding time at 30 sec and doping time for a minute, it means the substrate was first of the air dry at a minute at room temperature. The substrates were coated on both sides with different speeds per minute. The coated substrates were pre-heated at room temperature for minutes (air holding time) and 310 °C for 5 minutes. It was repeated at 12 times. The different coated samples as one coat, two coat, five coat, seven coat, ten coats, and 12 coats of different speeds per minute as 50mm/min, 150 mm/min, 250 mm/min, and 350 mm/min were post heated 400 °C for two hours at the rate of 22.5 °C/min on the hot furnace. Next working day to collect those samples of next day when they are naturally cooled at came on room temperature. A picture of a hot furnace is shown in figure 3.2.



Figure 3.2 Muffle furnace (Nabertherm: 30 °C – 3000 °C)[At Amrit research lab]

The processes of dip- coating are as shown in figure 3.3below.

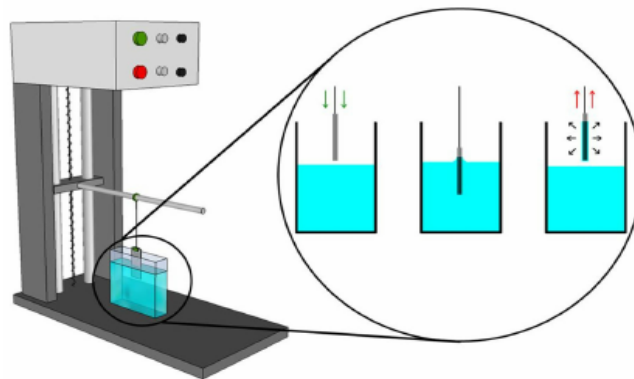


Figure 3.3 Schematic diagram of process of dip-coating [11]

In dip coating, the liquid film forms when a substrate undergoes the dip-coating process. The substrate is lowered into a bath of solution until it is mostly or fully immersed. A short delay occurs before the substrate is withdrawn. During the withdrawal process, a thin layer of the solution remains on the surface of the substrate. Once fully withdrawn, the liquid from the film begins to evaporate and leaves behind a dry film. Coating regimes ultimately determine the ‘thickness vs withdrawal speed’ behavior for a thin film. A further curing step can be performed; this forces the deposited material to undergo a chemical or physical change.

### 3.3 Sample Characterization

The optical characterization of the thin films was analyzed using UV-Vis spectrophotometer (HR4000CG UV-NIR, Ocean Optics). The optical characterization of the samples was performed in Amrit Campus (ASCOL) research lab. The transmittance and the band gap results were measured. A picture of the UV-Vis spectrophotometer is shown in figure 3.4,



Figure 3.4 UV-Vis spectrophotometer (HR4000CG UV-NIR, Ocean Optics) [At Amrit research lab]

### 3.4 Envelop Method (Swanepoel Method)

Among the various methods of finding the thickness of film the Swanepoel method is a method generally used for spectroscopic determination of optical properties of thin films using transmittance data. When thickness of the film is in the range of micrometer, some wave like patterns due to interaction of probe beam reflected from different interfaces appear in transmittance and reflectance spectrum. Swanepoel method can be used as a solution for this problem

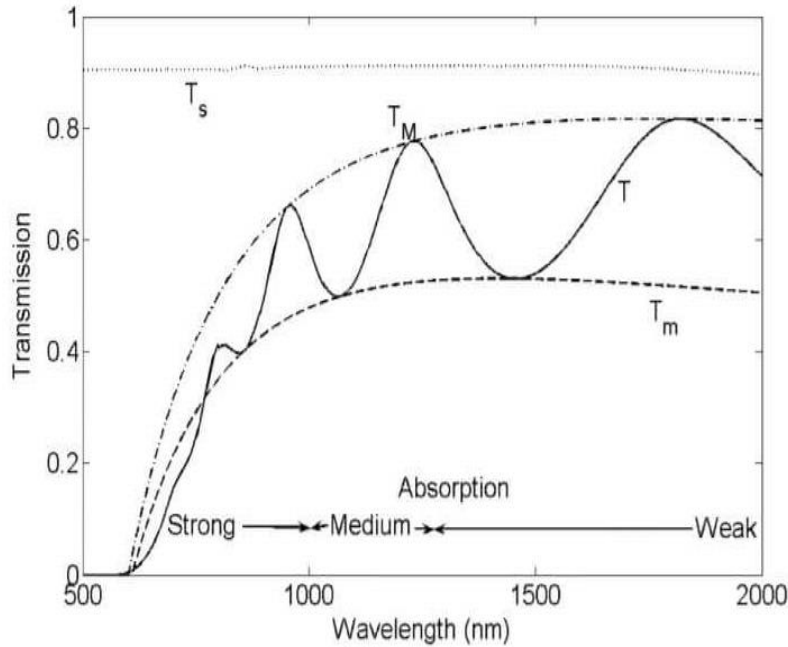


Figure 3.5 Envelope on the transmittance curve.  $T_{\max}$  and  $T_{\min}$  are the fitted curves to the maxima and minima of transmission spectrum [17]

### 3.5 Sensor Application

The sensitivity of the thin films was analyzed by homebuilt sensor setup. The sensitivity was measured in Research Laboratory of Physics, Amrit Campus. For the sensor applications, ethanol vapor was used as target gas. A heater made up of nickel- chromium wire was placed below the substrate to generate temperature up to 400 °C. The experimental set up of home-built gas sensor as shown in figure 3.6.



Figure 3.6 Homemade gas sensor set up [At Amrit research lab]

A thermocouple was placed in order to monitor the substrate temperature. A temperature controller was used to maintain the temperature inside the glass chamber. The electrical characteristics of the sensor were observed by changing the temperature from room to 31°C in air. After that, different concentrations of the ethanol vapor were supplied inside the glass chamber and its resistance variation with temperature was recorded. After injecting the gas inside the glass chamber, the chamber was made air tight by using the cork. After each injection of the gas, the gas was completely leaked out of the chamber and then, response time and recovery time was also measured. The resistance of the film was measured using a high mega-ohm multimeter. To measure gas response with gas sensor setup calculated using following relation:

$$R = \frac{R_a}{R_g} \quad (3.1)$$

The response of the gas sensor was calculated using following relation

$$\text{Sensitivity}(s) = \left( \frac{R_a - R_g}{R_a} \right) \times 100\% \quad (3.2)$$

Where,  $R_a$  is the resistance of the sensor measured in the air and  $R_g$  is the resistance in the presence of the target gas in the air [26]

## CHAPTER 4

### RESULTS AND DISCUSSION

In this section, the structural and optical characteristics of ZnO thin films prepared using a homebuilt dip coater have been summarized. The sensitivity response of the films has also been studied using a homebuilt sensor apparatus. The results of the experimental measurements are summarized in the following sections:

#### 4.1 Optical Properties

##### 4.1.1 Transmittance Analysis

The data are first measured from the UV-Vis spectrophotometer and the data obtained in the form of wavelength (nm) versus transmittance (%). The plot of transmittance versus wavelength is shown in fig 4.1

The UV-Vis optical transmittance of 0.5M ZnO thin film was measured in the wavelength of range (350 to 800) nm using a UV-Vis spectrophotometer. Figure 4.1 shows its optical transmittance which is more than 80% in (350 to 800) nm range.

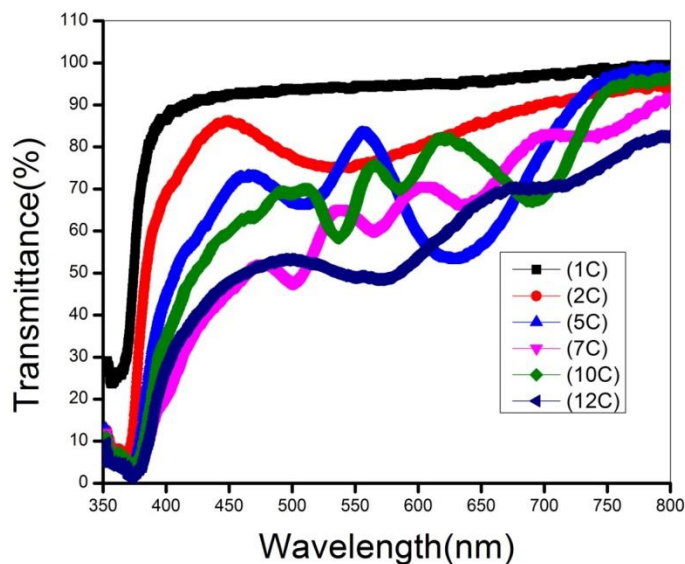


Figure 4.1 Transmittance for different ZnO Coat of 0.5M with speed 350mm/min.

Fig 4.1 shows that the wave length ranges 350 nm to 800 nm of different transmittance and from the graph it is clear to note that on increasing the higher coat, the transmittance was found to be decreased.

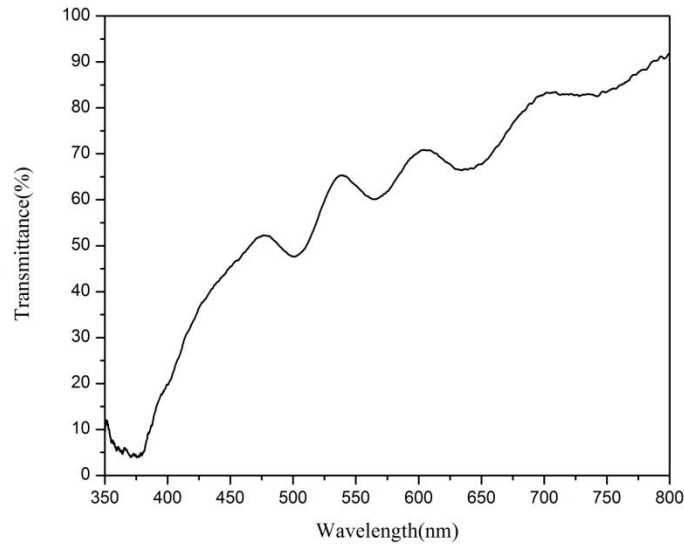


Figure 4.2 Transmittance for 0.5 M 7 Coat.

Figure 4.2 shows the transmittance of 7 coat ZnO samples. The optical properties ZnO thin films were studied in the wavelength range of 350 to 800 nm using UV-Vis spectrophotometer.

#### 4.1.2 Band gap Analysis

Figure 4.3 shows the Tauc plot of 0.5M ZnO of different coats, the direct band gap was calculated by extrapolating the linear portion of  $(\alpha h\nu)^2$  versus  $h\nu$  graph. The band gap was found to be 3.02 to 3.32 eV for different coats.

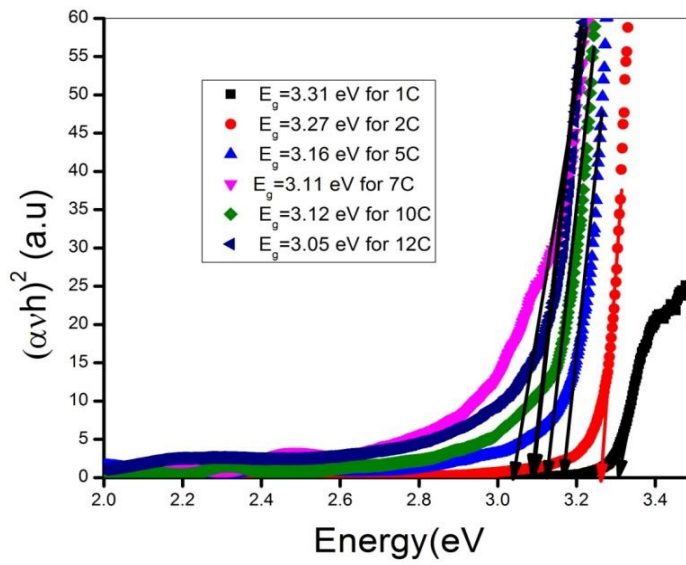


Figure 4.3 Band Gap of different coat

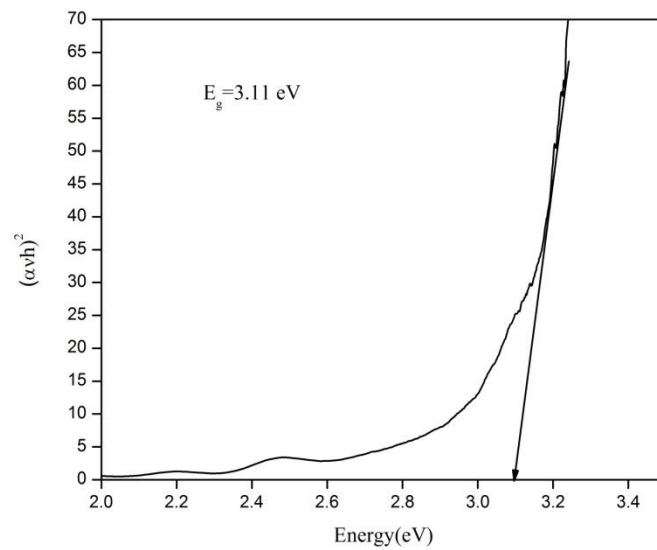


Figure 4.4 Band Gap of 7C coat ZnO.

Figure 4.9 Shows the Tauc plot of 0.5M ZnO, the direct bandgap was calculated by extrapolating the linear portion of  $(\alpha h\nu)^2$  versus  $h\nu$  graph. The bandgap was found to be 3.11 eV.

In Table 4.1, the band gap values of thin films identified using the Tauc plot of UV-Vis spectra are listed. These results are obtained by 0.5M concentrations of ZnO, variation with number of coatings and dipping speed and constant dipping time, and air holding time, pre-heat treatment and post-heat treatments.

Table 4.1 Band gaps observed for 0.5M ZnO solutions with variations of different dipping speed and numbers coats.

S. N.	Sample	Parameters applied on the substrate	Dipping Speed (mm/min)	Number of coats	Band Gap (eV)
1.	0.5M ZnO old	Dipping Time – 30 s Air Holding Time – 60 sec Pre-heat – 300 °C Post- heat – 400 °C	350	1	3.31
				2	3.27
				5	3.16
				7	3.11
				10	3.12
				12	3.05

### 4.1.3 Thickness Analysis

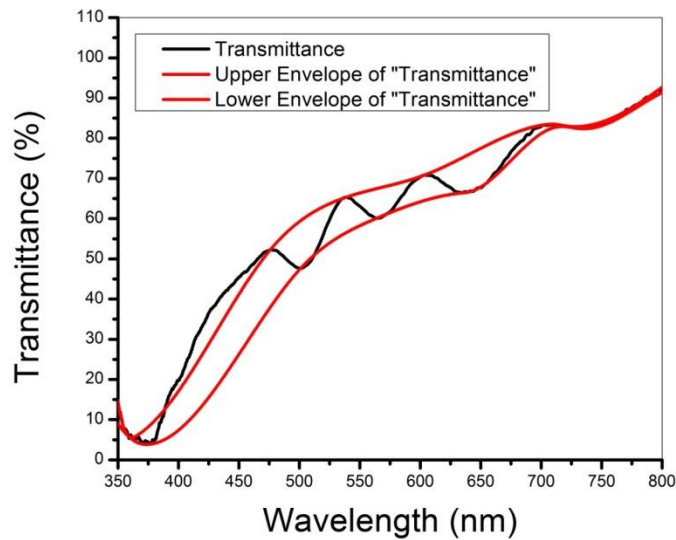


Figure 4.5 Envelope methods of ZnO thin film with 0.5 M of 7 Coat with speeds 350 mm/min.



The thickness of thin film can be calculated by using envelope methods suggested by Swanepoel applied to the film with higher thickness or maximum coat. By taking the account of two consecutive curves in the Transmittance spectra. Consider the two prominent peaks of T % versus the wavelength for maxima and minima has been calculated.

Table 4.2 The Values of  $\lambda$ ,  $T_{\max}$  and  $T_{\min}$  obtained from fig4. 5 and the  $n$  and  $d$  values calculated by Swanepoel method for 0.5M, 7 Coat ZnO thin film.

wavelength (nm)	Experimental				Theoretical			
	$T_{\max}$ (%)	$T_{\min}$ (%)	$n_1$	$d_1$ (nm)	$m_0$	$m$	$d_2$ (nm)	$n_2$
398.580	72.920	69.400	1.535	-	6.950	7	908.810	1.560
413.680	75.710	69.670	1.536	1258.820	6.700	6.5	875.290	1.563
443.710	83.250	73.930	1.533	952.740	6.240	6	868.310	1.561
483.970	86.020	75.450	1.543	845.960	5.750	5.5	862.550	1.569
536.750	87.280	78.480	1.537	729.360	5.170	5	873.040	1.565
613.740	89.290	81.240	1.536	729.000	4.520	4.5	899.030	1.564
705.320	93.800	85.000	1.536	-	3.930	4	918.380	1.563
Average				$d_{1(\text{avg})}=903.176$			$d_{2(\text{avg})}=886.480$	

Fig 4.5 the transmission curves ranging from 398.58 nm to 705.32 nm in the region the transmission curve is bunking up and down. The valley and tangent points are not same position there are a different of few nanometers. The calculation accuracy of  $n$  and  $d$  is more sensitive to values of  $\lambda$ ,  $T_M$  and  $T_m$  in the region of strong region. Swanepoel calculated the values of  $n$  and  $d$  by using the data of  $\lambda$ ,  $T_M$  and  $T_m$  at peaks value of the transmission curve.

Swanepoel method and the theoretical values  $n_2$ ,  $d_{2(\text{avg})}= 886.48= 1000$  nm and  $m$  respectively at the wavelengths of 398.58 nm to 705.32. However,  $n_1$ ,  $d_1$  and  $m_0$ calculated by envelop methods as shown in table4.2 are in good agreement with the theoretical values  $n_2$ ,  $d_{2(\text{avg})}= 886.48= 1000$  nm and  $m$  respectively. And after the interference order  $m_0$ is approached to  $m$  (integer or semi-integer),  $n_2$  and  $d_2$  are exactly consistent with their theoretical values.

The wavelength values are generally not an integer when the interference order  $m$ , the thickness  $d$  and the refractive index  $n$  are constants according to the interference equation 4.9

#### 4.1.4 Refractive index Analysis

The refractive index  $n$  is obtained by using Swanepoel methods as shown in figure 4.6, this shows that at the range of 350 nm – 800 nm of wave length range the refractive index was found to be 2.091–1.532. Below figure 4.3 shows that the refractive index varies at the region of 350nm – 500nm and constant at the region of 500nm -800nm.

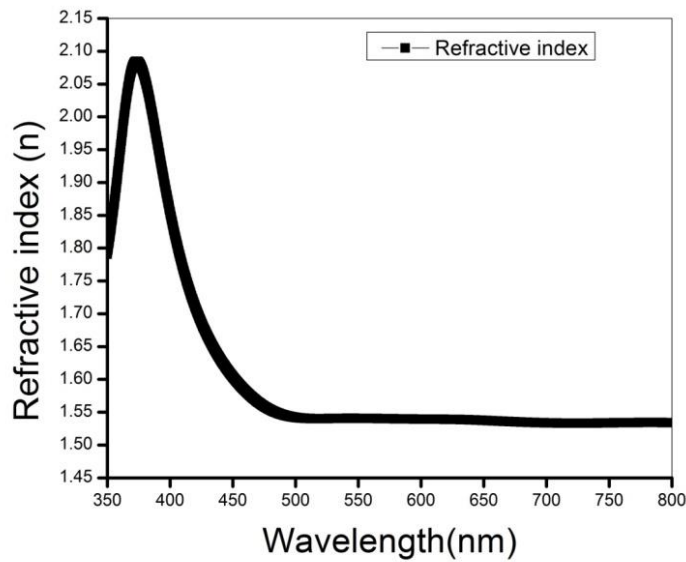


Figure 4.6 Refractive index

#### 4.1.5 Dielectric Constant Analysis

The extinction coefficient  $k$  is calculated using the following relation

$$k = \frac{\lambda \alpha}{4\pi} \quad (4.1)$$

The real and imaginary dielectric constant are calculated the formula for that is

For real,

$$\epsilon_r = 2nk \quad (4.2)$$

And imaginary,

$$\epsilon_r = n^2 - k^2 \quad (4.3)$$

The real versus wavelength, imaginary versus wavelength and both versus wavelength of graph is shown in fig below.

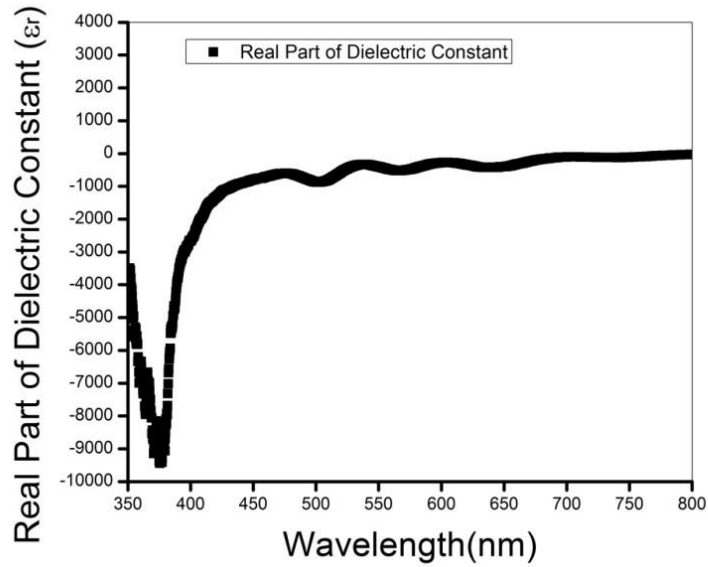


Figure 4.7 Real part of dielectric constant

The figure 4.7 shows that when the wavelength at the range of 360 nm to 380 nm the real part of dielectric constant is minimum and the range of wave length 380 nm to 400nm highly increase and the range of 400nm to 800m nm nearly constant of straight line.

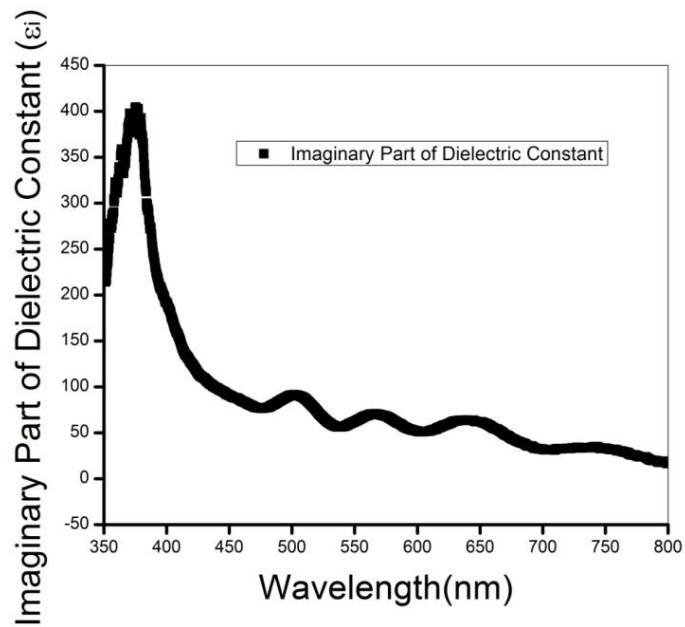


Figure 4.8 Imaginary part of dielectric constant

The figure 4.8 shows that when the wavelength at the range of 360 nm to 380 nm the imaginary part of dielectric constant is maximum and the range of wave length 380 nm to 400nm highly decrease and the range of 400nm to 800m nm nearly constant of straight line.

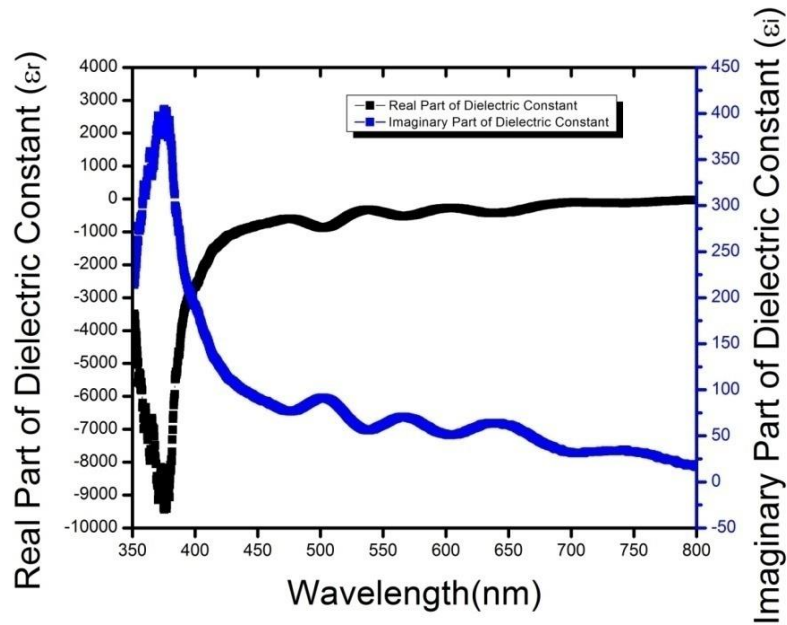


Figure 4.9 Real and imaginary part of dielectric constant

The figure 4.9 shows that the compression between two real and imaginary parts, here both parts are meeting at wave length 400 nm. After that meeting point, they become nearly constant of straight line.

## 4.2 Sensitivity Measurement

My research has been only focused on measuring the working temperature, response and recovery time.

### 4.2.1 Working Temperature Measurement

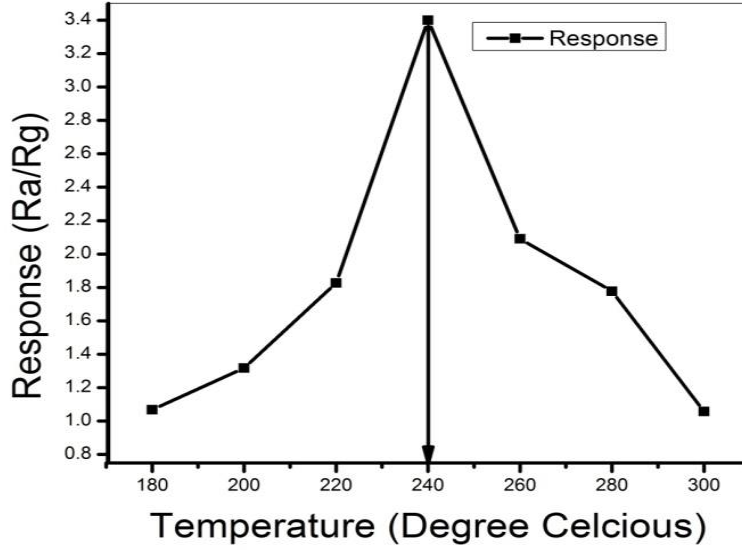


Figure 4.10 Working temperature of ZnO thin film for 500 ppm.

Figure 4.10 shows the working temperature for ZnO thin film for 7C, 0.5M for 500 ppm ethanol gas vapor using homemade gas sensor set up and the response was found to be at the temperature range from 180 °C to 300 °C. The result showed that highest response at temperature 240 °C. The resistances of at air and gas for different temperature are as shown in table 4.2.

Table 4.3 The working temperature of ZnO thin film for 7C, 0.5M for 500 ppm ethanol gas vapor.

Temperature °C	Resistance in air( $R_a$ ) ohm	Resistance in gas ( $R_g$ ) ohm	Response ( $R_a/R_g$ )
180	157.2	147.2	1.06793
200	79.6	60.4	1.31788
220	33.6	18.4	1.82609
240	20.4	6.0	3.40000
260	6.9	3.3	2.09091
280	1.6	0.9	1.77778
300	0.92	0.87	1.05747

## 4.2.2 Response and Recovery Time

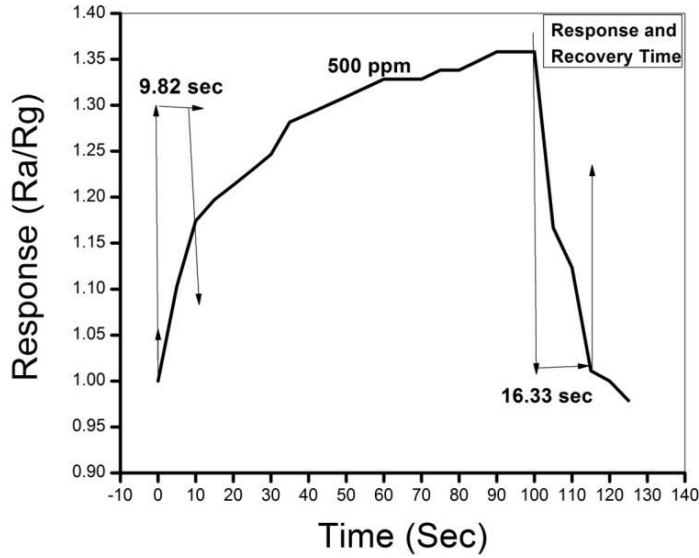


Figure 4.11 Responses and Recovery Time of ZnO sensor at 240°C on 500 ppm

Figure 4.11 shows that the response and recovery time of ZnO thin film for 7C, 0.5M for 500 ppm ethanol gas vapor using homemade gas sensor set up at the operating temperature 240 °C. The response time for first injection has been found to be 9.82 seconds and after 100 sec gases has been ejected, the recovery time was found to be 16.33 seconds.

## **CHAPTER 5**

### **CONCLUSIONS AND FUTURE WORK**

#### **5.1 Conclusions**

In this work, 6 samples of 0.5M ZnO films of different thickness had prepared by sol-gel dip-coating technique and optically characterized by using UV-Vis spectrophotometer. The thin film was prepared in 350mm/min speed. The average optical transmittance of all films was observed more than 80%. The band gap was observed 3.05 to 3.32 eV. Out of 6 samples we had chosen the best one is 0.5 M concentrations of 7 coats with 350 mm/min to studied on the basis of band gap found to be 3.11 eV, refractive index in the range of 2.091 -1.532 in the wavelength of 350-800 nm and the average thickness of the film was found to be 903.176 nm by using envelop method. The prepared ZnO thin film was used to detect ethanol vapor in temperature range 180 °C to 300 °C. The highest response 3.4 was found as operating temperature 240 °C for 500 ppm of ethanol vapor. The response and recovery time were found to be 9.82 and 16.33 sec for ethanol vapor.

#### **5.2 Future Work**

In future, following works can be done in our lab,

1. To make the porous thin film for high sensing response.
2. To measure the sensing at room temperature to investigate the sensitivity for other gases like LPG, Ammonia, Hydrogen, Nitrogen, etc.

## REFERENCES

- [1] H. Gong, J. Wang, C. H. Q. Hu, J. H. Ong and F. R. Zhu, *Sensors and Actuators B* **115**, 247 (2006).
- [2] M. Muniyandi, G. K. Mani, P. Shankar and J. B. B. Rayappan, , *Ceramics International* **40**, 7993 (2014)
- [3] E. R. Shabaan, I. S. Yahia and E. G. El-metwally, *Acta Physica Polonica A* **121**, 3(2012).
- [4] Y. Jin, B. Song, Z. Jia, Y. Zang, C. Lin, x. Wang and S.Dai, *Optics Express* **25**, 400(2017).
- [5] N. F. Habubi, N. A. Bakr and S. A. Salman, *Physical Chemistry An Indian Journal* **8**, 54(2013).
- [6] D. K. Chaudhari, R. Ghimere, S. P. Amatya, S. P. Shrestha and L. P. Joshi, *Junralof Physics Conference Series* **1706**, 012036(2020).
- [7] S. J. Chang, T. J. Hsueh, I. C. Chen and B. R. Huang, *Nanotechnology* **19**,175502 (2008).
- [8] S. M. Chou, L. G. Teoh, W. H. Lai, Y. H. Su and M. H. Hon, *sensors* **6**, 1420(2006).
- [9] K. Keis, C. Bauer, G. Bashloo, A. Hagfeldt, K. Westermark, H. Rensmo and H. Siegbahn, *Photochem. Photobiol. A* **148**, 57(2002).
- [10] J.E. Stehr, S.L. Chen, S. Filippov, M. Devika, N.K. Reddy, C.W. Tu, W.M. Chen and I.A. Buyanova, *AIP Conf. Proc.* **1583**, 272 (2014).
- [11] S. L. Chen, W. M. Chen and I. A. Buyanova, *Phys. Rev. B* **83**, 245212 (2011).
- [12] W. M. Chen, I. A. Buyanova, A. Murayama, T. Furuta, Y. Oka, D. P. Norton, S. J. Pearton, A. Osinsky and J. W. Dong, *Appl. Phys. Lett.* **92**, 92103 (2008).
- [13] M. Willander, L. L. Yang, A. Wadeasa, S. U. Ali, M. H. Asif, Q. X. Zhao and O. Nur, *J. Mater. Chem.* **19**, 1006 (2009).
- [14] M. H. Mamat, M. Z. Sahdan, Z. Khusaimi, A.Z. Ahmed, S. Abdullah and M. Rusop, *Optical Materials* **32**, 696(2010).
- [15] X. L. Cheng, H. Zhao, L. H. Huo, S. Gao and J. G. Zhao, *Sensors and Actuators B* **102**, 248(2004).
- [16] M. A. Kaid and A. Ashour, *Applied Surface Science* **253**, 3029(2007).
- [17] L. Jhu and W. Zeng, *A review Sensors and Actuators B* **116**, 1016(2017).
- [18] U. Alver, T. Kihnc, E. Bacaksiz, T. Kucukomeroglu, S. Nezir, I. H. Mutlu and F. Aslan, *Thin Solid Film.* **515**, 3448 (2007).
- [19] E. Backsiz, S. Aksu, S. Yilmz, M. parlak and M. Altunbas, *The Thin Films* **518**, 4076(2010).
- [20] C. Kittel, *Introduction to Solid State Physics*, Seventh Edition, John Wiley and Sons, New York, USA 199 (1986).



- [21] P. C. Chang, Z. Fan, D. Wang, W. Y. Tseng, W. A. Chiou, J. Hong and J. G. Lu, *Chem. Mater.* **16**, 5133 (2004)
- [22] M. C. Akgun, Y. E. Kalay and H.E Unalan, *Journals of Materials Research.* **27**, 1445(2012).
- [23] N. A. Alshehri, A. R. Lewis, C.P. Pearce and T. G. Maffei, *Journal of Saudi Chemical Society.* **22**, 538(2018).
- [24] C.S. Prajapati and P. P. Sahay, *Sensors and Actuators B: Chemica*, **169**, 1043(2011).
- [25] L. Wang, Y. Pu, Y. F. Chen, C. L. Mo, W. Q. Fang, C. B. Xiong, J. N. Dai and F. Y. Jiang, *J. Cryst. Growth.* **284**, 459 (2009).
- [26] M. H. Rahaman, U. Yaqoob, M. M. Uddin and H.C. Kim, *Applied Surface Science.* **549**, 14920(2014).
- [27] S. C. Ray, M. L. Karanjai, D. D. Gupta, *Thin Solid Films* **350**, 72 (1999).
- [28] N. Preda, M. Enculescu, I. Zgura, M. Socol, E. Matei, V. Vasilache and I. Enculescu, *Mater. Chem. Phys.* **138**, 253(2013).
- [29] M. Kumar, A. Kumar and A.C. Abhyankar, *Ceram. Int.* **50**, 1 (2014).
- [30] S. P. Shrestha, R. Ghimire, J.J. Nakarmi, Y.S. Kim, S. Shrestha, C. Y. Park and J. H. Boo, *Bull. Korean Chem. Soc.* **31**, 112 (2010).
- [31] S. S. Ahmed, E. K. Hassan and F. Emad, *Int. J. Phys. Research* **3**, 21 (2013).
- [32] N. K. Reddy and K. T. R. Reddy, *Mater. Res. Bull.* **41**, 414 (2006).
- [33] M. Kumar, A. Kumar and A.C. Abhyankar, *Ceram. Int.* **50**, 1 (2014).
- [34] H. U. Rashid, K. Yu, M. N. Umar, M. N. Anjum, K. Khan, N. Ahmad and M. T. Jan, *Rev. Adv. Mater. Sci.* **40**, 235 (2015).
- [35] C. Sima, W. Waldhauser, J. Lackner, M. Kahn, I. Nicolae, C. Viespe, C. Grigoriu and A. Manea, *J. Optoelectron. Adv. Mater.* **9**, 1446 (2007).
- [36] E. Morintale, C. Constantinescu and M. Dinescu, *Phys. AUC.* **20**, 43 (2010).
- [37] G. Bailly, A. Harrabi, J. Rossignol, B. Domenichini, J.P. Bellat, I. Bezverkhyy, P. Pribetich and D. Stuerza, *Procedia Engineering*, **168**, 264 (2016).
- [38] C. Liu, F. Yun and H. Morkoc, *J. Mater. Sci. - Mater. Electron.* **16**, 555 (2005).
- [39] H. E. Unalan, P. Hiralal, N. Rupesinghe, S. Dahal, W. I. Milne and G. A. J. Amaratunga, *Nanotech.* **19**, 1 (2008).
- [40] R. G. Aguilar and J. O. Lopez, *Lat. Am. J. Phys. Educ.* **5**, 368 (2011).
- [41] N. K. Reddy and K. T. R. Reddy, *Mater. Res. Bull.* **41**, 414 (2006).
- [42] P. R. Somani and S. Radhakrishnan, *J. Mater. Sci. - Mater. Electron.* **15**, 75 (2004).
- [43] S. A. Hooker, *Nanoparticles 2002 Conf. Proc.* **1** (2002).
- [44] B. B. Rao, *Mater. Chem. Phys.* **64**, 62 (2000).
- [45] M. Willander, L. L. Yang, A. Wadeasa, S. U. Ali, M. H. Asif, Q. X. Zhao and O. Nur, *J. Mater. Chem.* **19**, 1006 (2009).